Journal of Materials Chemistry C

Relationship between Molecular Structure of Uniquely Designed C2-symmetric Axially Chiral Dopants and Helical Twisting Properties of them in Cholesteric Liquid Crystals

Journal:	*Journal of Materials Chemistry C*
Manuscript ID	TC-ART-10-2018-005296.R1
Article Type:	Paper
Date Submitted by the Author:	03-Dec-2018
Complete List of Authors:	Yoshizawa, Daisuke; Kyushu University, Interdisciplinary Graduate School of Engineering Sciences Higuchi, Hiroki; Kyushu University, Institute for Materials Chemistry and Engineering Okumura, Yasushi; Kyushu University, Institute for Materials Chemistry and Engineering Kikuchi, Hirotsugu; Kyushu University, Institute for Materials Chemistry and Engineering

Journal Name

ARTICLE

Relationship between Molecular Structure of Uniquely Designed C2-symmetric Axially Chiral Dopants and Helical Twisting Properties of them in Cholesteric Liquid Crystals

Received 00th January 20xx,
Accepted 00th January 20xx

DOI: 10.1039/x0xx00000x

www.rsc.org/

Daisuke Yoshizawa, [a] Hiroki Higuchi, [b] Yasushi Okumura[b] and Hirotsugu Kikuchi[b]*

The induction of chirality in a liquid crystal (LC) can lead to the development of functional LC materials with enhanced properties. The chiral dopant is known to induce a molecular rearrangement and a subsequent helical twisting in the nematic LC host, affording a cholesteric liquid crystal (CLC). However, the chirality transfer mechanism has not been fully elucidated yet. In this study, we newly synthesized 9,9'-biphenanthrene-type chiral dopants ((*S*)-**2**s) following our work on binaphthyl-type chiral dopants with the aim of unveiling the chirality transfer mechanism. The molecular structures of the chiral dopants in the crystal were determined by XRD. The significantly unique Cotton effects was observed for (*S*)-**2**s, indicating that (*S*)-**2**s adopted different conformation in a solution from binaphthyl-type chiral dopants. Interestingly, one of (*S*)-**2**s shows positive temperature dependence of helical twisting power (HTP) though most chiral dopants show negative temperature dependence. The effects of mixing chiral dopants having opposite temperature dependence of helical twisting power were also investigated. Finally, the CLC showing temperature independency was achieved by mixing two types chiral dopants with reverse trend of temperature dependence in HTP.

1. Introduction

Chirality provides molecular compounds with attractive properties because, at molecular level, it can have an influence on the nano- to macro-scale self-organisation of molecules and, consequently, on their bulk functionality. Therefore, the introduction of chirality into a molecule often induces unique physical properties in materials.[1] For instance, the introduction of chirality into a liquid crystal (LC) has a tremendous impact on the arrangement of the LC molecules.[2] A nematic (N) LC changes to a cholesteric liquid crystal (CLC) with a helical structure by doping with a chiral molecule. The ability of a chiral dopant to induce a helical twisting with a molecular arrangement, the so-called helical twisting power (HTP_β), is defined according to the equation (1):

$$HTP_\beta = (p \cdot c \cdot r)^{-1} \quad (1)$$

where p is the helical pitch corresponding to the length along the helix over 2π molecular rotation of the director, c is the molar fraction of chiral dopant and r is the enantiomeric excess of chiral dopant. So far, a large number of chiral dopants with different chemical structures have been developed in order to investigate the relationship between their molecular structure and helical twisting properties.[3–11] Among them, binaphthalene derivatives have been shown to be promising candidates as chiral dopants because they have a relatively large helical twisting ability. Therefore, the strategic introduction of substituents into the binaphthalene skeleton can be expected to lead to functional LC materials with enhanced properties.[8–15]

In general, the structural similarity between a chiral dopant and the LC host enhances the solubility of the former and, with it, their intermolecular interaction.[3–5] Our group previously reported on a 6,6'-fluorinated binaphthyl-type chiral dopant that exhibited a large HTP value, good compatibility with a fluorinated LC host,[10] and enhancement of the temperature range of the blue phase.[15] Furthermore, the introduction of substituents has proven useful for the adjustment of the steric and electronic properties of the binaphthalene-type chiral dopants. In that work, to probe the effects of the interaction between the chiral dopant and the LC host on the helical twisting properties, we designed and synthesised a series of 6,6'-substituted bridged binaphthyl-type chiral dopants. We found that the binaphthyl-type chiral dopants having less bulkier and more polarisable substituents exhibited higher HTP values. In addition, the temperature dependence of the HTP values correlated well with the steric and polarisability properties of the substituents in the NLC host.[11]

Meanwhile, the length of the helical pitch tends to be sensitive to factors such as the molecular structure,[3–5] the optical purity,[16] the temperature,[2] and so on.[13,14,17–19] Thus, when the helical pitch is of the order of the visible wavelength, interference effects with visible light can be observed. Accordingly, these CLC materials exhibit selective reflection of circularly polarised light following Bragg's law, which corresponds to the length of the helical pitch. These unique properties render these materials potentially

[a] Interdisciplinary Graduate School of Engineering Sciences, Kyushu University, 6-1, Kasuga-koen, Kasuga, Fukuoka 816-8580, Japan
[b] Institute for Materials Chemistry and Engineering, Kyushu University, 6-1, Kasuga-koen, Kasuga, Fukuoka 816-8580, Japan. *E-mail: kikuchi@cm.kyushu-u.ac.jp
† Electronic Supplementary Information (ESI) available:

applicable as photonic materials such as tunable lasers due to photonic bandgap effects.[14,20–25] Concentration of a chiral dopant can also control the length of the helical pitch, allowing for selectively changing the colour of light. Therefore, chiral LC materials could find applications as colour-controllable devices.[26–29] On the other hand, the selective reflection of light from a CLC depends on the temperature, which explains the temperature dependency of the helical pitch of CLC. Some studies demonstrated single-pitched CLC systems using polymeric systems[30,31] or mixtures of chiral dopants.[32,33] However, the effect of the blend ratio of chiral dopants on the temperature dependence has not yet been fully elucidated. With the aim of unveiling the chirality transfer mechanism and the effect of mixing chiral dopants in a NLC host, which is considered as an important factor to develop CLC systems with variable temperature dependences, we herein describe the development of new chiral dopants, i.e. 9,9'-biphenanthrene derivatives, which were found to show positive temperature dependence of helical twisting ability.

2. Experimental section

2.1 Materials and instruments

All chemical reagents and solvents were obtained from commercial suppliers and were used without further purification. Analytical thin-layer chromatography (TLC) was performed on 0.25 mm E. Merck silica gel plates (silica gel F254); visualization with UV light (254 nm). Silica gel column chromatography was carried out with silica gel 60N from Wako Pure Chemical Industries (irregular, 63-212 μm). ^{1}H and ^{13}C NMR spectra were recorded on a JEOL JNM-LA400 spectrometer. Tetramethylsilane was used as an internal standard (δ 0.00) for ^{1}H and $CHCl_3$ (δ 77.06) for ^{13}C. Coupling constants, *J*, were reported in hertz (Hz). High-performance liquid chromatography (HPLC) was conducted on a Shimazu Corporation with Daicel CHIRALPAK IA-3 column (parameters given in each description). UV-vis absorptions were measured on a Shimazu 3150 spectrometer. CD spectra were recorded on a JASCO J-720W spectropolarimeter. Mass spectra and Elemental analysis were carried out by Kyushu University. X-ray diffraction measurements were carried out on a Rigaku R-AXIS RAPID diffractometer or a Rigaku FR-E+ diffractometer and graphite-monochromated Cu-Kα radiation (λ = 1.5419 A°) or Mo-Kα radiation (λ = 0.71075 A°). As a host nematic liquid crystals, a mixture of fluorinated nematic liquid crystals, (JC-1041XX, JNC Co. Ltd.) / 4-cyano-4'-pentyl biphenyl (5CB, Aidrich) = 1/1 (mol/mol) was used. Optical textures of samples were observed under the cross nicol with a polarising optical microscope (POM; Nikon, ECLIPSE E600 PDL). The temperature of sample was precisely controlled by a hot stage (Linkam, LTS-E350) in which the temperature can be controlled by a temperature controller (Linkam, 10013L) with an accuracy of ± 0.1 °C. To measure of a helical pitch of chiral nematic phase, a wedge cell, of which the inner surfaces were coated with polyimide thin film and rubbed in parallel to give a homogeneous liquid crystal alignment, was used (tan ϑ = 0.0079° ± 10 %) (E.H.C. Co.).

2.2 Synthesis

Synthesis of (*S*)-**2-OEt**. (*S*)-**2-OH** (156 mg, 0.40 mmol), potassium carbonate (383 mg, 2.8 mmol), sodium iodide (6.0 mg, 0.040 mmol), and bromoethane (0.53 mg, 4.8 mmol) were dissolved in acetone (10 mL) at room temperature under N_2, and mixture was heated to reflux for 2 days. After cooling to room temperature, the reaction mixture was poured into water and extracted with CH_2Cl_2 (20 mL). The separated organic layer was washed with water (10 mL x 2) and brine (10 mL x 2). The collected organic layer was dried over Na_2SO_4, filtrate, and evaporation to give a crude product, which was purified by recrystallization from EtOH to yield (*S*)-**2-OEt** (153 mg, 86 % with > 99 % ee) as white solid. ^{1}H NMR (400 MHz, $CDCl_3$) δ: 8.83 (2H, d, *J* = 7.7 Hz), 8.77 (2H, d, *J* = 8.2 Hz), 8.38 (2H, dd, *J* = 8.2, *J* = 1.4 Hz), 7.74 (4H, m), 7.55 (2H, m), 7.31 (4H, q, *J* = 1.8 Hz), 3.85 (2H, m), 3.60 (2H, m), 0.95 (6H, t, *J* = 7.0 Hz), ^{13}C NMR (100 MHz, $CDCl_3$) δ: 152.4, 150.1, 133.2, 131.8, 127.1, 126.90, 126.85, 126.7, 125.3, 123.8, 122.8, 122.6, 69.6, 15.7, MS(EI): m/z = 442 (M^+). Elemental analysis calcd (%) for $C_{32}H_{26}O_2$: C 86.85, H 5.92; found: C 86.55, H 5.97. The enantiomeric excess of (*S*)-**2-OEt** was determined by chiral phase HPLC (Daicel CHIRALPAK IA-3, hexanes/*i*-PrOH 1:1, flow rate 0.25 mL min^{-1}, 30 °C) minor enantiomer t_R = 17.63 min.

3. Results and Discussion

3.1 Synthesis and structural characteristics of the chiral dopants

We prepared two types of C2-symmetric axially chiral binaphthyl ((*S*)-**1**s) and biphenanthryl ((*S*)-**2**s) dopants (Fig. 1). The preparation of the chiral compound **2-OH** was carried out via a slightly modified literature procedure.[34–36] Then, the ethoxylation of (*S*)-**2-OH** gave (*S*)-**2-OEt**. The details of the synthesis and structural characteristics of the chiral dopants are described in the Experimental section and

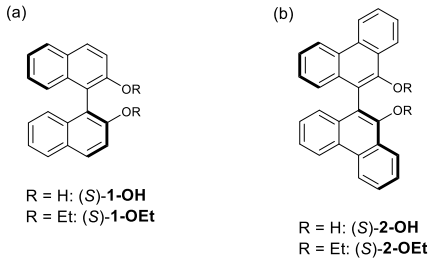

Fig. 1 Chemical structures of chiral dopants with axial chirality. (a) (*S*)-binaphthyl-type chiral dopants **1** and (b) (*S*)-biphenanthryl-type chiral dopants **2**.

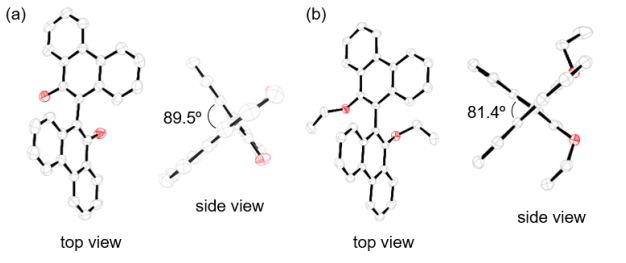

Fig. 2 ORTEP drawings of (a) (*S*)-**2-OH** and (b) (*S*)-**2-OEt** with thermal ellipsoids shown at the 50% probability level. All hydrogen atoms and THF molecules in (a) are omitted for clarify.

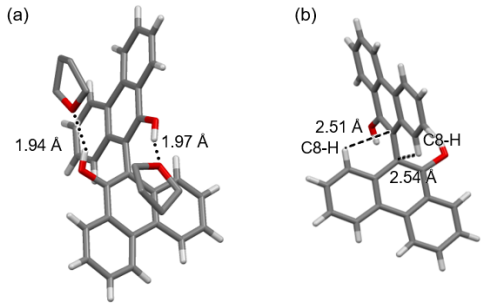

Fig. 3 Crystal structure of (*S*)-**2-OH**. (a) Dotted lines indicate hydrogen bonding. (b) Dashed lines indicate the intramolecular edge-to-face interactions. THF molecules are omitted for clarify.

Supporting information.

When the dihedral angle (ϑ) between the two aromatic rings of (*S*)-binaphthalene or (*S*)-biphenanthrene derivatives is 0° < ϑ < 90°, they adopt a *cisoid* conformation, whereas with a dihedral angle ϑ > 90° the conformation is *transoid*. As a first step to clarify the relationship between the helical structure of the induced CLC and the molecular structure of the chiral dopants, we investigated the conformation of the latter. Thus, the molecular structures of (*S*)-**2**s were determined by X-ray crystallography and compared with those of (*S*)-**1**s, which were reported elsewhere. Fig. 2 shows the ORTEP representations of (*S*)-**2-OH** and (*S*)-**2-OEt**. The structural analysis revealed that the dihedral angle (ϑ) of (*S*)-**1-OH** was 76.4°, characteristic of the *cisoid* conformation. On the other hand, (*S*)-**1-OEt** adopted the *transoid* conformation (ϑ = 111.9°). As shown in Fig. 3 (a), the crystal of (*S*)-**2-OH** included two solvent THF molecules, whose oxygen atoms formed hydrogen bonds with the hydroxyl groups of the phenanthrol moieties (1.94 and 1.97 Å, respectively) (Fig. 3 (a), dotted line). The distances between the proton at the C8 position of each phenanthrene ring and the bridging C9 atom of the other ring were 2.51 and 2.54 Å, respectively (Fig. 3 (b), dashed line). It is known that the aromatic rings often serve as acceptors of C–H hydrogen because the π-systems have low-energy LUMOs and polarisable electrons occupying the HOMOs.[37] Therefore, the π-systems can act as good electron-donating groups.[38–40] The phenanthrene backbone with large fused rings often exhibits edge-to-face interactions.[41–43] Accordingly, the C8-H protons of the phenanthrene rings and the C9 carbons could also be involved in intramolecular edge-to-face interactions. These results suggest that both edge-to-face and hydrogen bonding interactions contribute to maintain the *quasi-orthogonal* conformation (ϑ = 89.5°) in (*S*)-**2-OH**. In contrast, (*S*)-**2-OEt** exhibits longer C8-H…C9 distances (2.54 and 2.56 Å, respectively), which indicates that the intramolecular interaction in (*S*)-**2-OEt** is smaller than that of (*S*)-**2-OH**, most likely due to the flexibility of the ethoxy moieties forcing the *cisoid* conformation (ϑ = 81.4°).

3.2 UV–vis absorption, photoluminescence spectra and circular dichroism (CD) spectra of chiral dopants

Fig. 4 (a) and (b) show the UV–vis absorption and photoluminescence spectra, respectively, of the chiral dopants in acetonitrile.

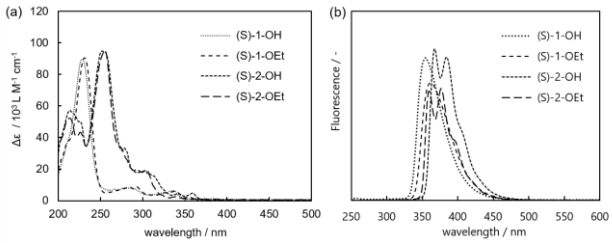

Fig. 4 (a) UV–vis absorption (5.0 x 10^{-6} mol L^{-1}, rt) and (b) photoluminescence spectra of chiral dopants (5.0 x 10^{-5} mmol L^{-1}, rt; (*S*)-**1-OH**, λ_{ex} = 228 nm; (*S*)-**1-OEt**, λ_{ex} = 232 nm; (*S*)-**2-OH**, λ_{ex} = 252 nm; (*S*)-**2-OEt**, λ_{ex} = 256 nm).

The UV–vis absorption bands of (*S*)-**1-OH** and (*S*)-**1-OEt** at 228 and 232 nm, respectively, corresponds to the binaphthalene ^1B_b transition with a long axis polarisation, and those in the ranges of 250–300 and 300–350 nm correspond to the ^1L_a and ^1L_b transitions, respectively. The spectra of (*S*)-**2**s display a substantial red-shift absorbance relative to (*S*)-**1**s that is attributable to the wide-spread π-conjugation of the phenanthrene rings in (*S*)-**2**s compared to that of the naphthalene rings of (*S*)-**1**s. The UV–vis absorption peaks that appear at 214 nm in the spectra of (*S*)-**2-OH** and (*S*)-**2-OEt** can be assigned to the ^1C_b transition, and those at 252 and 256 nm are attributable to the ^1B_b transition with a long axis polarisation of the phenanthrene ring. Furthermore, the absorption peaks at 270–330 and 330–400 nm stem from the ^1L_a and ^1L_b transitions, respectively.[44,45]

The photoluminescence spectra of (*S*)-**1**s and (*S*)-**2**s show Stokes shifts. Compounds (*S*)-**1-OH** and (*S*)-**1-OEt** exhibit photoluminescence at 355 and 361 nm, respectively. Meanwhile, the replacement of the naphthalene rings of the binaphthyl-type chiral dopants with phenanthrene rings induce two photoluminescence peaks at 367 and 387 nm for (*S*)-**2-OH** and 359 and 376 nm for (*S*)-**2-OEt**. Dopants (*S*)-**2**s exhibit red-shifted emission compared to (*S*)-**1**s, despite the long-wavelength excitation light. These results indicate that (*S*)-**2**s have the potential to be used as blue light emitter materials.

Fig. 5 shows CD spectra of the chiral dopants in acetonitrile. The CD spectra of binaphthalene derivatives are known to depend on the value of the dihedral angle (ϑ) between the two chromophores according to the exciton coupling theory.[46] The (*S*)-binaphthalene derivatives exhibit a positive CD couplet for ϑ in the range from 0° to 100°, and a negative one from 110° to 180° at the naphthalene absorption (^1B_b transition). In the CD spectra of (*S*)-**1s**, the same Cotton effects that has been previously reported for other

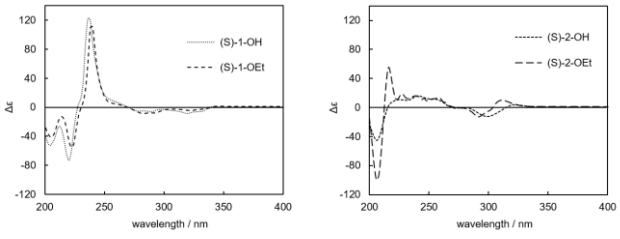

Fig. 5 CD spectra of chiral dopants (5.0 x 10^{-5} mol L^{-1}, rt)

analogues is observed,[9,47] i.e. strong bisignated Cotton effects around 230 nm and weak Cotton effects at –350 nm, which are respectively assigned to the ^1B_b, ^1L_a and ^1L_b transitions. In addition, the spectra of (*S*)-**1**s show a positive CD couplet in the region of the ^1B_b transition, indicating that these compounds adopt the *cisoid* conformation in isotropic solvents such as acetonitrile. In contrast, the CD spectra of (*S*)-**2**s are considerably different. The weak Cotton effects at 340, 300 and 250 nm can be assigned to the ^1L_a, ^1L_b and ^1B_b transitions, respectively; a strong positive couplet corresponding to the ^1C_b band is observed for (*S*)-**2-OEt**, whereas (*S*)-**2-OH** shows no couplet in the range of the ^1C_b transition. As a consequence, it should be expected that both compounds adopt different conformations in isotropic solvents. Several studies have estimated the conformation of biphenanthrene derivatives in isotropic solvents using the CD couplet of the phenanthrene chromophore. Thus, (*R*)-1,1'-biphenanthrene derivatives showed a positive couplet for the ^1B_b band, which opposite in sign to that was obtained by the exciton chirality method for the phenanthrene chromophore.[48] In the case of (*R*)-4,4'-biphenanthrene backbones, a negative couplet corresponding to the ^1B_b transition was observed, which was in agreement with computational calculations.[49] These discrepancies were ascribed to the overlap with other electronic transitions of the phenanthrene chromophore.[45] The correlations between the CD couplet and the conformation of the biphenanthrene backbone have not been clarified in detail so far.

3.3 Helical twisting properties of chiral dopants in NLC

The helical twisting property of CLC with a binaphthyl-type chiral dopant is governed by the conformation of the chiral dopant (*cisoid* or *transoid*). We determined the twisting direction (the helical sense) of the CLC through the contact method using cholesterol oleyl carbonate (COC) as a standard left-handed LC. The contact method was performed on the basis of the observation of the contact area between COC and the prepared CLC. The optical textures of both phases would be expected to merge continuously throughout the contact region if CLC and COC had the same helical sense. As shown in Fig. 6 (b) and (d), a continuous area can be observed between the CLC with (*S*)-**1-OEt** or (*S*)-**2-OEt** and COC, indicating that both dopants induced the formation of left-handed CLCs. On the other hand, a discontinuous boundary appeared between the CLC with (*S*)-**1-OH** or (*S*)-**2-OH** and COC (Fig. 6 (a) and (c), respectively). The stable conformations of the chiral dopants, obtained by single crystal analysis, and the twisting direction of the CLCs are summarised in Table 1. For the chiral binaphthalene dopants, the dopant with *cisoid* conformation induced the opposite helical sense than the *transoid* dopant. The (*R*)-1,1'-binaphthalene dopants bearing ethoxy substituents at 2,2'-positions in the binaphthalene rings showed positive Cotton effects in the range of 250 nm in NLC solvent, indicating that they adopted the *transoid* conformation in NLC solvents and induced the generation of right-handed CLC.[9] Therefore, the conformation of (*S*)-**1-OEt** in NLC can be assigned as *transoid*, the same as in the crystal. In contrast, (*S*)-**1-OH** and (*S*)-**2-OH** adopted the *cisoid* conformation in NLC, since they induced the right-handed conformation in the CLC. This result suggests that (*S*)-**2-OH** adopted the same *cisoid* conformation in NLC as in the crystal due to the intramolecular edge-to-face interactions of the phenanthrene rings described above. However, (*S*)-**2-OEt** induced the left-handed conformation in CLC despite the fact that the crystal-packing effects caused the *cisoid* conformation in the crystal of (*S*)-**2-OEt**. This result implies that the expanded condensed rings of (*S*)-**2-OEt** render it easily influenced by the liquid-like fluidity of the NLC solvent due to the flexibility of its conformation in the absence of intramolecular interactions such as edge-to-face interaction.

Table 1 Helical twisting properties of (*S*)-**1**s and (*S*)-**2**s in NLC

chiral dopant	conformation in crystal	twisting direction of CLC
(*S*)-**1-OH**	*cisoid*	right
(*S*)-**1-OEt**	*transoid*	left
(*S*)-**2-OH**	*cisoid* (*quasi-orthogonal*)	right
(*S*)-**2-OEt**	*cisoid*	left

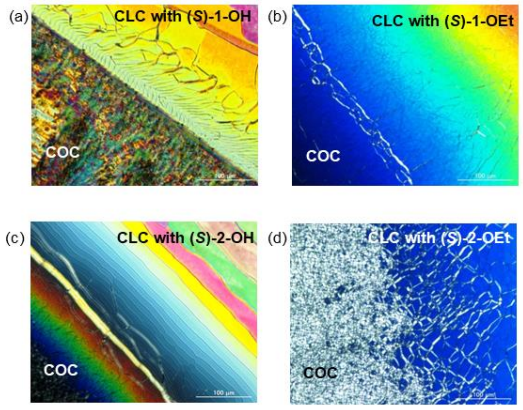

Fig. 6 Polarised optical micrographs of contact tests between COC and the CLC with the corresponding chiral dopant in JC1041-XX/5CB (equimolar mixture) at 35 °C: (a) CLC with (*S*)-**1-OH**, (b) CLC with (*S*)-**1-OEt**, (c) CLC with (*S*)-**2-OH**, (d) CLC with (*S*)-**2-OEt**.

Fig. 7 shows the temperature dependence of the absolute value of HTP_β ($|HTP_\beta|$) for CLC with the corresponding chiral dopant. The $|HTP_\beta|$ values of (*S*)-**1**s and (*S*)-**2**s in the host NLC were evaluated by using the Cano wedge cell method,[50] which is based on the observation of striped disclination lines by polarised optical microscopy (POM). The disclination of the helical structure of CLC occurs when the cell gap increases continuously along the wedge because the wedged-cell has been treated to produce homogenous alignment. The helical pitch (*p*) of the CLC can be determined from

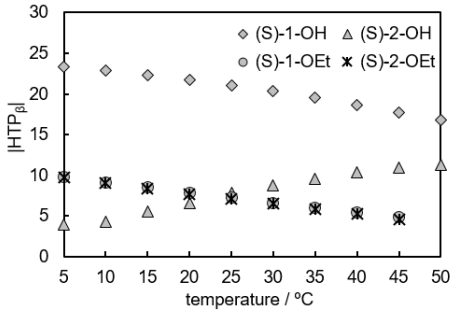

Fig. 7 Temperature dependences of $|HTP_\beta|$s for CLC with (*S*)-**1**s and (*S*)-**2**s.

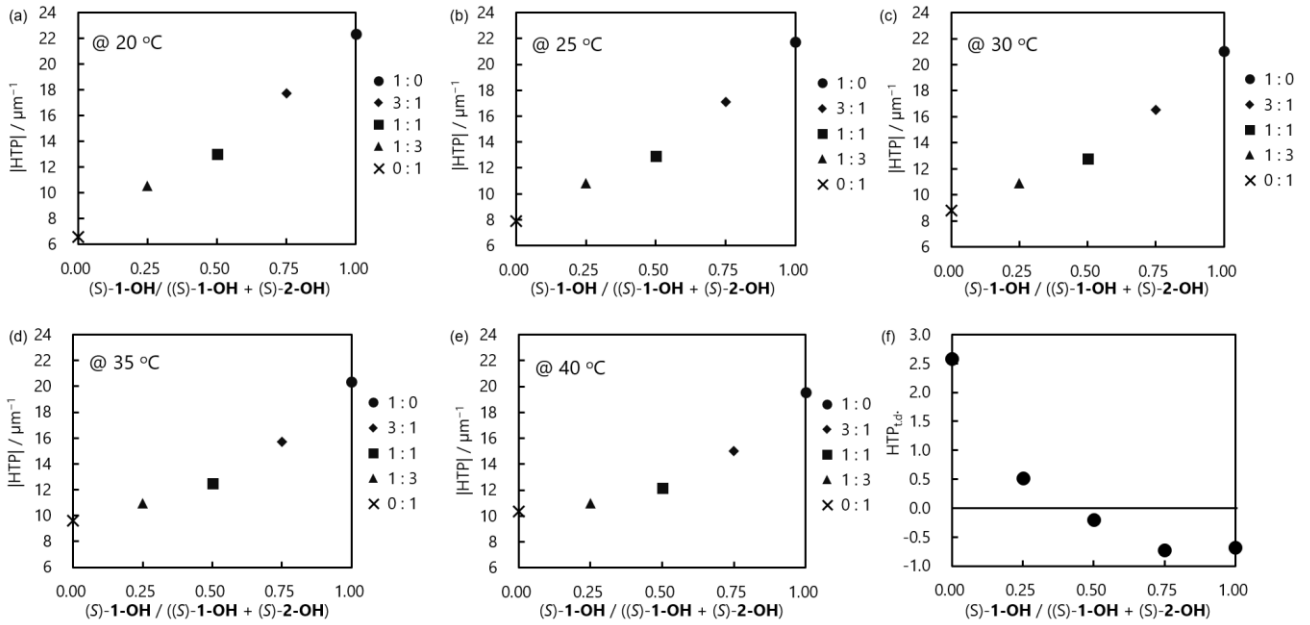

Fig. 8 (a) – (e) Temperature and concentration dependences of the CLCs doped with (*S*)-**1-OH** and (*S*)-**2-OH** and (f) plots of the $HTP_{t.d.}$ values.

the wedged angle (ϑ) of the cell and the distance between the striped disclination lines (L) according to the following equation (2):

$$p = 2\mathrm{L}\tan\theta. \quad (2)$$

Dihedral angles between the two aromatic rings of the binaphthalene derivatives around 45° or 135° would be expected to afford the largest |HTP| values, whereas it is zero at dihedral angles around 0° or 90°.[12] The large $|HTP_\beta|$ value of (*S*)-**1-OH** could be caused by the conformational rigidity of the intramolecular hydrogen bonding between the two hydroxyl groups.[12] In contrast, the enhanced molecular flexibility introduced by the ethoxy groups caused a decrease of the $|HTP_\beta|$ values in (*S*)-**1-OEt**. The same trend was observed for (*S*)-**2-OEt**. Furthermore, as the temperature increased, a significant decrease in $|HTP_\beta|$ was observed for (*S*)-**1-OH**, (*S*)-**1-OEt** and (*S*)-**2-OEt**. The helical pitch of CLC strongly depends on the conformation of the chiral dopant. In general, the helical pitch of the NLC increases with the temperature, that is, the helical twisting ability of the chiral dopant decreases because the suitable conformation of the chiral dopant varies with temperature. However, (*S*)-**2-OH** exhibited smaller $|HTP_\beta|$ value than the other dopants in the low temperature region. Moreover, interestingly, the helical twisting ability of (*S*)-**2-OH** increased with the temperature, which contrasts with the trend observed for the other chiral dopants. These results suggest that the stable conformation of (*S*)-**2-OH** with edge-to-face intramolecular interactions affords low helical twisting ability. In addition, its *quasi-orthogonal* conformation seemingly changed with increasing temperature. It seems reasonable to conclude that non-covalent bonds such as those involved in intramolecular edge-to-face (CH…π) interactions of the chiral dopants are effective despite the temperature dependency and provide unique chiral properties in the NLC host.

To investigate the effect of using a mixture of chiral dopants on the NLC host, the two chiral dopants that show opposite temperature dependency, (*S*)-**1-OH** and (*S*)-**2-OH**, were dissolved in the NLC host, and the mixing ratio dependence of HTP was measured. It is known that the effect is a linear function of the concentration of chiral dopant in dilute solutions, and the chiral induction of the HTP can be described in a good approximation as

$$\mathrm{HTP} = \sum_i x_i (HTP)_i, \quad (3)$$

where x_i is the mole fraction and $(HTP)_i$ is the HTP of the species *i*. The HTP has to be correlated to a partial molar quantity.[51] Figure 8 shows the temperature dependences of the CLCs with different concentrations of the mixed chiral dopants. The mole fractions of zero and one indicate the original HTP values of (*S*)-**2-OH** and (*S*)-**1-OH**, respectively. As shown in Figures 8 (a)–(e), HTP exhibited good linear relation with the mole fraction of chiral dopants in the low temperature region, whereas a poor linearity was gradually observed in the high temperature region, indicating that equation (3) does not always hold. Then, we evaluated the temperature dependence of the HTP in detail, which is calculated by equation (4);[10]

$$\mathrm{HTP_{t.d.}} = (\Delta\mathrm{HTP} / \overline{\mathrm{HTP}}) / \Delta\mathrm{T} \times 100, \quad (4)$$

where ΔHTP is the difference between the maximum and the minimum |HTP| values in a measured temperature range (over 40 °C in this study), and $\overline{\mathrm{HTP}}$ is the arithmetic mean of |HTP| in the same temperature range. The index means the amount of change of |HTP| per 1 °C. Although, according to equation (3), the relation between $HTP_{t.d.}$ and the molar ratio of (*S*)-**1-OH** and (*S*)-**2-OH** should be linear, the plot of the experimental results deviated from the linearity and was concave downward for a given molar ratio as shown in Figure 8 (f). The reason for the difference between the

theoretical and experimental results is still unclear, and further investigations are required for clarification. Finally, the CLC doped with an equimolar fraction of chiral dopants exhibited an almost constant value of HTP over a wide temperature range, that is, a nearly zero $HTP_{t.d.}$, which suggests that a CLC with a temperature independent pitch was actually achieved. This is due to (*S*)-**2-OH** and (*S*)-**1-OH** having similar structures while opposite temperature dependence of helical twisting power. The single-pitched CLC was realised by mixing chiral dopants with reverse trend of HTP temperature dependence in an appropriate ratio, which resulted in the cancelling of dopant-induced helical twisting effects with the same direction.

4. Conclusions

We have synthesised new chiral dopants, the (*S*)-9,9'-biphenanthrene derivatives (*S*)-**2-OH** and (*S*)-**2-OEt**, and their helical twisting properties, as well as those of related binaphthyl derivatives (*S*)-**1-OH** and (*S*)-**1-OEt**, have been evaluated for the induction of a CLC from a NLC host. Intramolecular edge-to-face interactions were observed for (*S*)-**2-OH**, which adopted a *quasi-orthogonal* conformation in the crystalline state. Dopants (*S*)-**2**s showed almost the same absorbance and photoluminescence emission spectra due to their structural similarities based on the 9,9'-biphenanthrene backbone. However, their CD spectra were found to differ significantly from each other in the range of the ^1C_b band, which suggests that (*S*)-**2**s adopted different conformation in an isotropic solvent. A temperature dependency of the CLC and a significant decrease in $|HTP_\beta|$ with increasing temperature were observed for (*S*)-**1-OH**, (*S*)-**1-OEt** and (*S*)-**2-OEt**. However, the $|HTP_\beta|$ value in the low temperature ranges for (*S*)-**2-OH** was vanishingly small, whereas it was found to increase with the temperature, which is in sharp contrast with the trend observed for the other chiral dopants. This can be envisaged as a result of the difference in the intramolecular interactions, i.e. the presence or absence of edge-to-face interaction. We also investigated the effects of mixing chiral dopants having opposite temperature dependence of helical twisting power on the resulting CLC. The mixtures of (*S*)-**1-OH** and (*S*)-**2-OH** in the NLC host exhibited good correlation between HTP and mole fraction in the low temperature region, whereas gradually poor linearity was observed with increasing temperature. Finally, a single-pitched CLC was achieved by mixing appropriate fractions of (*S*)-**1-OH** and (*S*)-**2-OH** through the cancelling of dopant-induced helical twisting effects with the same direction. We believe that the results herein presented constitute an important contribution to the elucidation of the chirality transfer mechanism and the future design of new chiral dopants with unique chirality properties.

Acknowledgements

This work was partially supported by a Grant-in-Aid for Scientific Research (A) JSPS KAKENHI Grant Number JP25248021 and 18H03920 from the Japan Society for the Promotion of Science, Dynamic Alliance for Open Innovation Bridging Human, Environment and Materials from the Ministry of Education, Culture, Sports, Science and Technology, Japan (MEXT), the Cooperative Research Program of "Network Joint Research Center for Materials and Devices." and CREST, JST (JPMJCR1424).

Conflicts of interest

There are no conflicts to declare.

Notes and References

1 C. Tschierske, in *Chirality at the Nanoscale*, ed. D. B. Amabilino, Wiley-VCH Verlag GmbH & Co. KGaA, Weinheim, Germany, 2009, pp. 271–304.
2 H.-S. Kitzerow and C. Bahr, in *Chirality in Liquid Crystals*, eds. H.-S. Kitzerow and C. Bahr, Springer-Verlag, New York, pp. 1–27.
3 R. Eelkema and B. L. Feringa, *Org. Biomol. Chem.*, 2006, **4**, 3729–3745.
4 S. Pieraccini, S. Masiero, A. Ferrarini and G. Piero Spada, *Chem. Soc. Rev.*, 2011, **40**, 258–271.
5 N. Katsonis, E. Lacaze and A. Ferrarini, *J. Mater. Chem.*, 2012, **22**, 7088–7097.
6 G. Gottarelli, G. P. Spada, M. Hibert, R. Zimmermann, G. Solladie and B. Samori, *J. Am. Chem. Soc.*, 1983, **105**, 7318–7321.
7 A. Ferrarini, G. Moro and P. Nordio, *Phys. Rev. E*, 1996, **53**, 681–688.
8 M. Goh and K. Akagi, *Liq. Cryst.*, 2008, **35**, 953–965.
9 T. Mori, M. Kyotani and K. Akagi, *Macromolecules*, 2008, **41**, 607–613.
10 K. Kakisaka, H. Higuchi, Y. Okumura and H. Kikuchi, *Chem. Lett.*, 2014, **43**, 624–625.
11 Y. Narazaki, H. Nishikawa, H. Higuchi, Y. Okumura and H. Kikuchi, *RSC Adv.*, 2018, **8**, 971–979.
12 G. Proni, G. P. Spada, C. Organica, P. Lustenberger, R. Welti and C.- Zu, *J. Org. Chem.*, 2000, 5522–5527.
13 A. Saha, Y. Tanaka, Y. Han, C. M. W. Bastiaansen, D. J. Broer and R. P. Sijbesma, *Chem. Commun.*, 2012, **48**, 4579–4581.
14 H. Nishikawa, D. Mochizuki, H. Higuchi, Y. Okumura and H. Kikuchi, *ChemistryOpen*, 2017, **6**, 684.
15 K. Kakisaka, H. Higuchi, Y. Okumura and H. Kikuchi, *J. Mater. Chem. C*, 2014, **2**, 6467–6470.
16 G. Solladié and R. G. Zimmermann, *Angew. Chemie Int. Ed. English*, 1984, **23**, 348–362.
17 R. Eelkema and B. L. Feringa, *Org. Lett.*, 2006, **8**, 1331–1334.
18 R. Eelkema, M. M. Pollard, J. Vicario, N. Katsonis, B. S. Ramon, C. W. M. Bastiaansen, D. J. Broer and B. L. Feringa, *Nature*, 2006, **440**, 163.
19 X. Su, S. Voskian, R. P. Hughes and I. Aprahamian, *Angew. Chemie Int. Ed.*, 2013, **52**, 10734–10739.
20 H. K. Bisoyi and Q. Li, *Acc. Chem. Res.*, 2014, **47**, 3184–3195.
21 H. K. Bisoyi and Q. Li, *Chem. Rev.*, 2016, **116**, 15089–15166.
22 S. Furumi, S. Yokoyama, A. Otomo and S. Mashiko, *Appl. Phys. Lett.*, 2003, **82**, 16–18.
23 S. M. Morris, P. J. W. Hands, S. Findeisen-tandel, R. H. Cole, T. D. Wilkinson and H. J. Coles, *Opt. Express*, 2008, **16**, 2503–2507.
24 S. Yokoyama, S. Mashiko, H. Kikuchi, K. Uchida and T. Nagamura, *Adv. Mater.*, 2006, **18**, 48–51.
25 Y. Inoue, H. Yoshida, K. Inoue, Y. Shiozaki, H. Kubo, A. Fujii and M. Ozaki, *Adv. Mater.*, 2011, **23**, 5498–5501.
26 N. Tamaoki, A. V. Parfenov, A. Masaki and H. Matsuda, *Adv. Mater.*, 1997, **9**, 1102–1104.
27 N. Tamaoki, *Adv. Mater.*, 2001, **13**, 1135–1147.

28 F. Castles, F. V. Day, S. M. Morris, D.-H. Ko, D. J. Gardiner, M. M. Qasim, S. Nosheen, P. J. W. Hands, S. S. Choi, R. H. Friend and H. J. Coles, *Nat. Mater.*, 2012, **11**, 599–603.
29 S. Tokunaga, Y. Itoh, Y. Yaguchi, H. Tanaka, F. Araoka, H. Takezoe and T. Aida, *Adv. Mater.*, 2016, **28**, 4077–4083.
30 N. Y. Ha, Y. Ohtsuka, S. M. Jeong, S. Nishimura, G. Suzaki, Y. Takanishi, K. Ishikawa and H. Takezoe, *Nat. Mater.*, 2008, **7**, 43–47.
31 R. Balamurugan and J.-H. Liu, *React. Funct. Polym.*, 2016, **105**, 9–34.
32 Y. J. Liu, P. C. Wu and W. Lee, *Mol. Cryst. Liq. Cryst.*, 2014, **596**, 37–44.
33 K. S. Shim, J. U. Heo, S. I. Jo, Y.-J. Lee, H.-R. Kim, J.-H. Kim and C.-J. Yu, *Opt. Express*, 2014, **22**, 15467.
34 R. L. Kidwell, M. Murphy and S. D. Darling, *Org. Synth.*, 1969, **49**, 90.
35 J. Aydin, K. S. Kumar, M. J. Sayah, O. A. Wallner and K. J. Szabó, *J. Org. Chem.*, 2007, **72**, 4689–4697.
36 D. W. Norman, C. A. Carraz, D. J. Hyett, P. G. Pringle, J. B. Sweeney, A. G. Orpen, H. Phetmung and R. L. Wingad, *J. Am. Chem. Soc.*, 2008, **130**, 6840–6847.
37 M. Nishio, M. Hirota and Y. Umezawa, *The CH-[pi] interaction : evidence, nature, and consequences*, Wiley, New York, 1998.
38 Y. Umezawa, S. Tsuboyama, K. Honda, J. Uzawa and M. Nishio, *Bull. Chem. Soc. Jpn.*, 1998, 71, 1208–1214.
39 O. Takahashi, Y. Kohno and M. Nishio, *Chem. Rev.*, 2010, **110**, 6049–6076.
40 M. Nishio, *Phys. Chem. Chem. Phys.*, 2011, **13**, 13873–13900.
41 Y. Imai, S. Kido, K. Kamon, T. Kinuta, T. Sato, N. Tajima, R. Kuroda and Y. Matsubara, *Org. Lett.*, 2007, **9**, 5047–5050.
42 T. Ukegawa, T. Kinuta, T. Sato, N. Tajima, R. Kuroda, Y. Matsubara and Y. Imai, *Tetrahedron*, 2010, **66**, 8756–8762.
43 Y. Kitayama, T. Amako, N. Suzuki, M. Fujiki and Y. Imai, *Org. Biomol. Chem.*, 2014, **12**, 4342–4346.
44 A. Solladié-Cavallo, C. Marsol, G. Pescitelli, L. D. Bari, P. Salvadori, X. Huang, N. Fujioka, N. Berova, X. Cao, T. B. Freedman and L. A. Nafié, *European J. Org. Chem.*, 2002, **2002**, 1788–1796.
45 P. L. Polavarapu, in *Chiroptical Spectroscopy: Fundamentals and Applications*, Taylor & Francis, New York, 2016, pp. 232–234.
46 S. F. Mason, R. H. Seal and D. R. Roberts, *Tetrahedron*, 1974, **30**, 1671–1682.
47 D. Ishikawa, T. Mori, Y. Yonamine, W. Nakanishi, D. L. Cheung, J. P. Hill and K. Ariga, *Angew. Chemie Int. Ed.*, 2015, **54**, 8988–8991.
48 T. Hattori, K. Sakurai, N. Koike, S. Miyano, H. Goto, F. Ishiya and N. Harada, *J. Am. Chem. Soc.*, 1998, **120**, 9086–9087.
49 G. Gottarelli, G. Proni, G. P. Spada, D. Fabbri, S. Gladiali and C. Rosini, *J. Org. Chem.*, 1996, **61**, 2013–2019.
50 I. Dierking, *Textures of Liquid Crystals*, Wiley-VCH Verlag GmbH & Co. KGaA, Weinheim, FRG, 2003.
51 H.-G. Kuball and T. Höfer, in *Chirality in Liquid Crystals*, Springer-Verlag, New York, pp. 67–100.